APPPOLO: A Brazilian Processing Software for Multi-GNSS Precise Point Positioning

João Pedro Voltare Zaupa[1], Daniele Barroca Marra Alves[1], Paulo de Tarso Setti Jr[2]

[1]Faculty of Science and Technology, São Paulo State University - Unesp, Presidente Prudente, SP, Brazil – jp.zaupa@unesp.br; daniele.barroca@unesp.br

[2]Center for Weather Forecasting and Climate Studies, National Institute for Space Research – CPTEC/INPE, Cachoeira Paulista, SP, Brazil – paulo.setti@inpe.br

Keywords: Multi-GNSS, Precise Point Positioning, Convergence Time.

Abstract

This paper presents the development and evaluation of a Brazilian software for Precise Point Positioning (PPP) using multiple Global Navigation Satellite Systems (GNSS). The tool, named APPPOLO (Advanced Precise Point Positioning software for Optimized Localization), was designed to support advanced modeling and flexible configuration for academic and applied research in GNSS positioning. A specific performance analysis was conducted focusing on multi-GNSS PPP solutions using data from Brazilian continuously operating GNSS stations. The assessment examined the impact of different GNSS constellation combinations on positional accuracy and convergence time. The results demonstrate significant improvements in both accuracy and convergence when integrating GPS, GLONASS, Galileo, and BeiDou, compared to standalone systems. This paper contributes to ongoing efforts to develop robust, locally adapted GNSS processing tools capable of addressing atmospheric and infrastructural challenges found in South America.

1. Introduction

Precise Point Positioning (PPP) is a well-established GNSS technique capable of achieving centimeter-level accuracy using a single receiver and precise satellite products (Zumberge et al., 1997; Kouba et al., 2017). Since its introduction in the 1990s, PPP has evolved significantly, supporting a wide range of scientific, commercial, and operational applications (Choy et al., 2017). In recent years, the growing availability of signals from multiple GNSS constellations (GPS, GLONASS, Galileo, and BeiDou) has enhanced PPP performance by increasing the number of simultaneously tracked satellites, improving spatial geometry, and reducing the time required for solution convergence (Montenbruck et al., 2017; Glaner and Weber, 2023).

Numerous software packages have been developed to implement PPP solutions, including open-source options such as RTKLIB (Takasu, 2012), PPPH (Bahadur and Nohutcu, 2018), GAMP (Zhou et al., 2018), PPPLib (Chen and Chang, 2021), MG-APP (Xiao et al., 2020), SUPREME (Zhao et al., 2021), PRIDE PPP-AR (Geng et al., 2019), and raPPPid (Glaner and Weber, 2023). These tools vary in strengths, from ambiguity resolution and real-time capability to user interface design and support for low-cost receivers. However, challenges persist regarding software accessibility, flexibility for educational use, integration of Brazilian GNSS data, and adaptation to the intense atmospheric variability typical of low-latitude regions.

In response to this need, the software APPPOLO (Advanced Precise Point Positioning software for Optimized Localization) was developed within an academic setting in Brazil (Zaupa, 2025). It provides a user-friendly, modular, and highly configurable environment for multi-GNSS PPP processing. APPPOLO includes support for common GNSS data formats, advanced correction models (e.g., phase center offsets, atmospheric delays), and a graphical interface tailored for research and teaching. Unlike many existing tools, it was specifically designed to handle data from the Brazilian Network for Continuous Monitoring of the GNSS Systems (RBMC) and enable systematic performance assessments under local conditions. In addition, APPPOLO was deliberately conceived as a modular and adaptable platform, supporting both advanced research applications and educational use in undergraduate and graduate geoscience programs. Furthermore, the software has the potential to be distributed to the broader community, extending its impact beyond the academic environment in which it was originally developed.

This paper introduces APPPOLO and evaluates its performance in static PPP mode, focusing on the impact of different constellation combinations and on session times in the afternoon (local time). The analysis is based on real GNSS data from RBMC stations and aims to verify the potential benefits of multi-GNSS integration in the Brazilian context. The following sections detail the methodology, processing configuration, and results related to positional accuracy and convergence behavior.

2. Software Architecture

The APPPOLO software was developed in MATLAB and designed with a modular structure, allowing users to configure the processing environment flexibly. It supports the main RINEX formats and provides compatibility with auxiliary files such as SP3 (precise orbits), CLK (satellite clocks), ANTEX (antenna calibrations), EOP (Earth Orientation Parameters) and OSB (Observable-Specific Bias). The software includes a graphical user interface (GUI) that facilitates the selection of constellations (GPS, GLONASS, Galileo, BeiDou), frequencies, and observation types (Table 1), including code (C), carrier phase (L), Doppler (D), and signal-to-noise ratio (S) when available. Users can activate or deactivate correction models such as satellite and receiver antenna phase center offsets and variations, solid Earth tides, ocean loading, pole tide, relativistic effects, and phase wind-up. Atmospheric models include Hopfield or Saastamoinen (hydrostatic delay), Askne & Nordius (wet component), and Niell or GMF (Global Mapping Function) mapping functions.

The estimation algorithm is based on an extended Kalman filter (EKF) that integrates dual-frequency (IF) code and carrier-phase observations. The filter estimates receiver coordinates, neutrospheric delay, receiver clock offset, and float ambiguities.

This contribution has been peer-reviewed. The double-blind peer-review was conducted on the basis of the full paper.
https://doi.org/10.5194/isprs-annals-X-3-W4-2025-379-2026

Quality control routines, such as cycle slip detection, elevation angle-based weighting, and outlier rejection, are also incorporated (Zhang et al., 2018).

System	Frequency 1	Frequency 2	Frequency 3+
GPS	L1C, L1P, L1W, L1Y, L1M, L1N	L2C, L2P, L2W, L2Y, L2M	L5I, L5Q, L5X
GLONASS	L1C, L1P	L2C, L2P	L3I, L3Q, L3X, L4A, L4B, L4X, L6A, L6B
Galileo	L1A, L1B, L1C, L1X, L1Z	L5I, L5Q, L5X (E5a), L7I, L7Q, L7X (E5b)	L6A, L6B, L6C, L6X, L6Z, L8I, L8Q, L8X
BeiDou	B1I (C2I), B1C (C1C), B1A (C1A)	B2I (C7I), B2a (C5I), B2b (C6I)	B3I (C3I), B3A (C8I), B3Q (C8Q)

Table 1. Supported GNSS Observation Codes by System and Frequency. Source: Adapted from Romero (2021) and Zaupa (2025).

The overall structure of the processing chain is illustrated in Figure 1, which summarizes the main functional blocks.

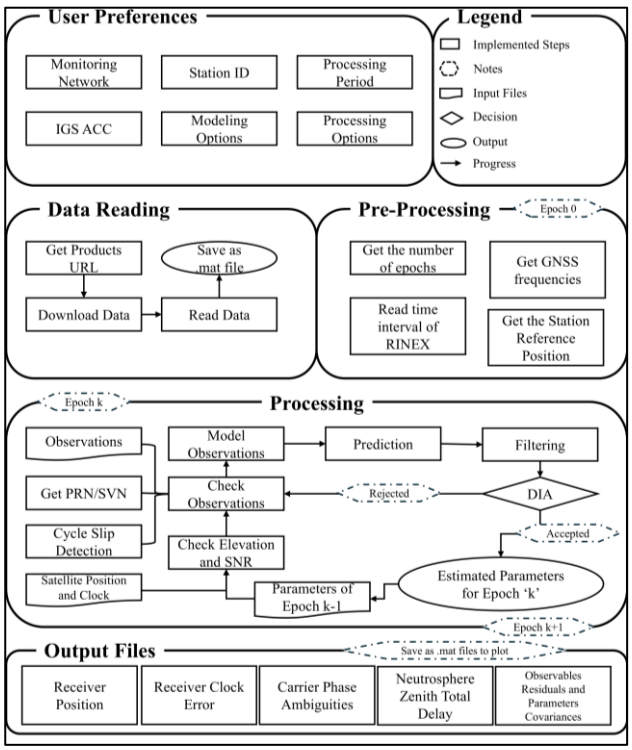

Figure 1. Workflow of APPPOLO software.

3. Precise Point Positioning

The PPP technique implemented in APPPOLO uses dual-frequency pseudorange and carrier-phase observations combined with precise satellite products. The approach allows absolute positioning without the need for a reference station, relying instead on accurate modeling of signal propagation and satellite-receiver geometry.

The observation model adopted is based on the IF linear combination (Equations 1 and 2), which eliminates first-order ionospheric delay. The linearized equations for pseudorange and carrier-phase observations are given by Equations 3 and 4 (Kouba et al., 2017):

$$P_{IF} = \frac{{f_1}^2}{({f_1}^2-{f_2}^2)}P_1 - \frac{f_2^2}{({f_1}^2-{f_2}^2)}P_2, \quad (1)$$

$$\varphi_{IF} = \frac{{f_1}^2}{({f_1}^2-{f_2}^2)}\varphi_1 - \frac{f_2^2}{({f_1}^2-{f_2}^2)}\varphi_2, \quad (2)$$

$$P_{IF} = \rho + c\left(\delta t_{r,G} - \delta t^s\right) + m_f Zwd + \epsilon, \quad (3)$$

$$\varphi_{IF} = \rho + c\left(\delta t_{r,G} - \delta t^s\right) + m_f Zwd + N_{IF} + \varepsilon, \quad (4)$$

where P_{IF} = IF of pseudoranges observations P_1, P_2 for frequencies f_1 and f_2, respectively (m)
φ_{IF} = IF of carrier phase observations φ_1, φ_2 for frequencies f_1 and f_2, respectively (m)
ρ = the geometric distance between receiver and satellite (m)
$c\left(\delta t_{r,G} - \delta t^s\right)$ = accounts for receiver 'r' and satellite 's' clock errors for a constellation 'G' (m)
m_f = neutrospheric mapping function
Zwd = zenith wet delay (m)
N_{IF} = carrier-phase ambiguity term (m)
ϵ, ε = measurement noise and unmodeled errors of pseudorange and carrier phase, respectively.

In addition to the classical first- and second-frequency IF combination, APPPOLO also allows the use of alternative frequency pairs, such as the first and third, second and third, or even higher-order combinations like the fourth and fifth frequencies available in Galileo and BeiDou systems. This flexibility enables advanced analyses under different ionospheric conditions and supports modern multi-frequency constellations for optimized PPP performance.

The Kalman filter in APPPOLO estimates the receiver coordinates, zenith wet delay, receiver clock offset, and float ambiguities. To generalize the observation model for multi-constellation PPP, the linearized functional model can be expressed in matrix form as:

$$y = Ax + Bb + e, \quad (5)$$

where y = vector of IF observation residuals
x = vector of unknown parameters
b = vector of auxiliary parameters such as inter-system biases (ISBs)
A, B = design matrices for x and b, respectively
e = vector of measurement errors and residuals.

This generalized structure enables the simultaneous estimation of parameters for all visible satellites and constellations, while accounting for system-specific biases and constellation-dependent behavior.

The EKF estimation process sequentially updates the state vector at each epoch using both prediction and correction steps (Zaupa, 2025). The measurement noise $\sigma^2_{f,obs}$ are modeled through covariance matrices defined a priori, based on empirical values and signal elevation angles:

$$\sigma^2_{f,obs} = \sigma^2_{0,f,obs}(\sin E)^{-2} \quad (6)$$

where E is the satellite elevation angle, and $\sigma^2_{0,f,obs}$ is an empirical constant. For pseudorange observations, values of 0.8 m (f_1) and 1.0 m (f_2) are adopted; for carrier-phase observations, values of 0.008 m (f_1) and 0.01 m (f_2) are used (Veettil et al., 2020). These values reflect typical performance of geodetic-level receivers and are suitable for computing the IF combination. According to the law of variance propagation, the variance of the IF observable $\sigma^2_{IF,obs}$ is given by (Parvazi et al., 2023):

$$\sigma^2_{IF,obs} = \left(\frac{f_1^2}{(f_1^2-f_2^2)}\right)^2 \sigma^2_{f_1,obs} + \left(\frac{f_2^2}{(f_1^2-f_2^2)}\right)^2 \sigma^2_{f_2,obs}\,. \qquad (7)$$

This formulation defines the diagonal elements of the observation covariance matrix, which is used in the Kalman filter update step to weight both code and phase measurements accordingly. The EKF structure in APPPOLO allows flexible configuration of the state vector. The receiver coordinates and phase ambiguities are modeled as constants (treated as white noise in case of cycle slips) throughout each session, while the residual component of the zenith wet delay is estimated as a random walk process. The receiver clock offset per constellation is treated as a white noise process, and the neutrospheric delay is incorporated via mapping functions applied to the Zwd. Quality control routines are integrated throughout the processing chain, including cycle slip detection based on the TurboEdit Algorithm (Blewitt, 1990), residual outlier exclusion using statistical thresholds, and redundancy-based checks for solution integrity (Zhang et al., 2018).

4. Experimental Setups and Evaluation Strategy

The experimental stage was designed to evaluate the performance of APPPOLO under different GNSS constellation configurations. A total of 15 combinations were analyzed, classified into four groups: single-constellation (GPS - G, GLONASS - R, Galileo - E, and BeiDou - C), dual-constellation (e.g., GR, EC), triple-constellation (e.g., GEC), and the full four-system combination (GREC). This strategy aimed to assess how the PPP solution behaves under different multi-GNSS configurations and session lengths. Data from three RBMC stations were selected: PPTE, POAL, and TOPL. These stations provide high-quality GNSS data and are geographically distributed to represent different atmospheric and geometry conditions across Brazil (Figure 2).

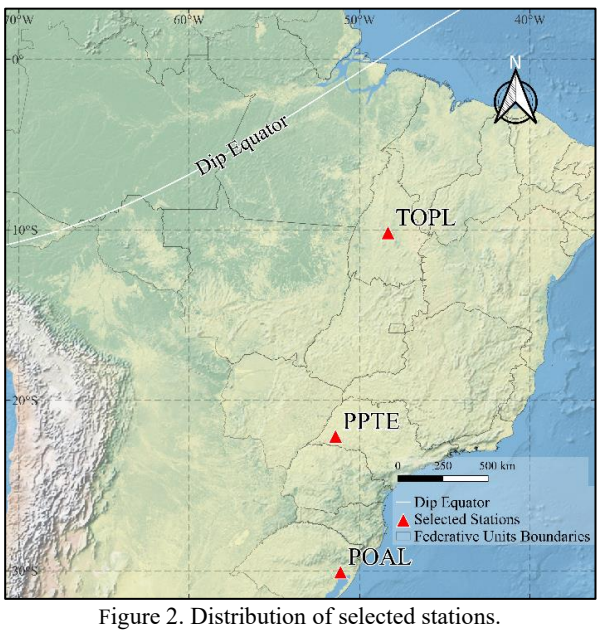

Figure 2. Distribution of selected stations.

The evaluation focused on two performance metrics:

- The average three-dimensional positional accuracy over different time spans: 30 minutes, 1 hour, 2 hours, and 4 hours;
- The convergence time of the PPP solution in both horizontal and vertical components.

All processing sessions were initialized at 14:00 local time (UTC−3). Table 2 summarizes the configuration adopted for this PPP processing experiments using APPPOLO.

Parameter	Configuration
Observables	GPS: C1C + C2W / L1C + L2W; GLONASS: C1P + C2P / L1P + L2P; Galileo: C1X + C5X / L1X + L5X; BeiDou: C2I + C6I / L2I + L6I;
Estimator	Extendend Kalman Filtering + Quality Control
Masks	Elevation > 10; SNR > 29; Positional Diluition of Position (PDOP) < 6
Orbits and Clocks	CODE SP3 (orbits) and CLK (clocks) products
OSB Products	Wuhan University
Coordinates & Ambiguities	Estimated as constant (white noise for ambiguities during cycle slips)
Receiver Clock Offset	Estimated as white noise
Zenith Wet Delay	Estimated as random walk
Other Systematic Effects	Phase wind-up, Sagnac effect, relativistic and EOP corrections, Phase Center Offsets and Variations

Table 2. Processing configuration adopted in this experiment.

Additionally, the average satellite visibility per constellation was analyzed across the three stations to contextualize expected PPP performance under each configuration and session length. Figure 3 presents the average number of satellites observed per constellation. These numbers reveal that station TOPL had the highest satellite visibility for both the GPS and Galileo systems. Specifically, the average number of GPS satellites was 11 at PPTE, 10 at POAL, and 13 at TOPL. For GLONASS, the average was 7 in all three stations. Galileo showed consistent values at PPTE and POAL (7 satellites) and higher visibility at TOPL (9). BeiDou, in turn, showed the greatest temporal and inter-station variation, with drops in the number of tracked satellites and high PDOP peaks, especially at PPTE (8 satellites on average) and POAL (5 satellites). At TOPL, the average was 5 satellites. This discrepancy is associated with differences in receiver firmware: PPTE is equipped with a Trimble Alloy receiver, while POAL and TOPL operate with Trimble NetR9 receivers, which offer limited support for full BeiDou tracking.

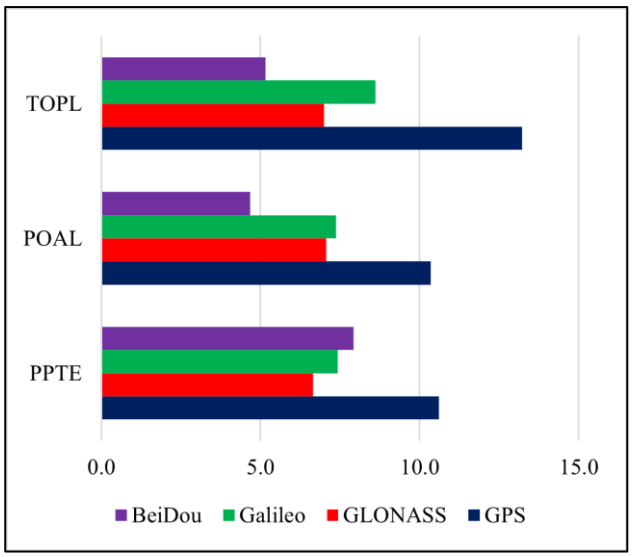

Figure 3. Average number of tracked satellites for each constellation and monitoring station.

5. Results and Discussion

5.1 Positional Accuracy

The average 3D positional accuracy was assessed over four different time spans: 30 minutes, 1 hour, 2 hours, and 4 hours, across all GNSS constellation configurations and the three selected stations (PPTE, POAL, and TOPL). These metrics provide a robust indication of how the PPP solution improves over time and how it responds to different combinations of GNSS systems.

The evolution of 3D positional accuracy (discrepancy and standard deviation) for all GNSS constellation combinations at PPTE, POAL, and TOPL stations is shown in Figure 4. The solutions are grouped into single-, dual-, triple-, and quadruple-constellation configurations. The discrepancy values were computed based the known reference coordinates at each station. As expected, accuracy improves with longer observation periods and with the inclusion of multiple GNSS constellations. The benefits of multi-GNSS integration are particularly evident in the shorter sessions (30 min and 1 h), where configurations involving three or four systems show significantly reduced errors.

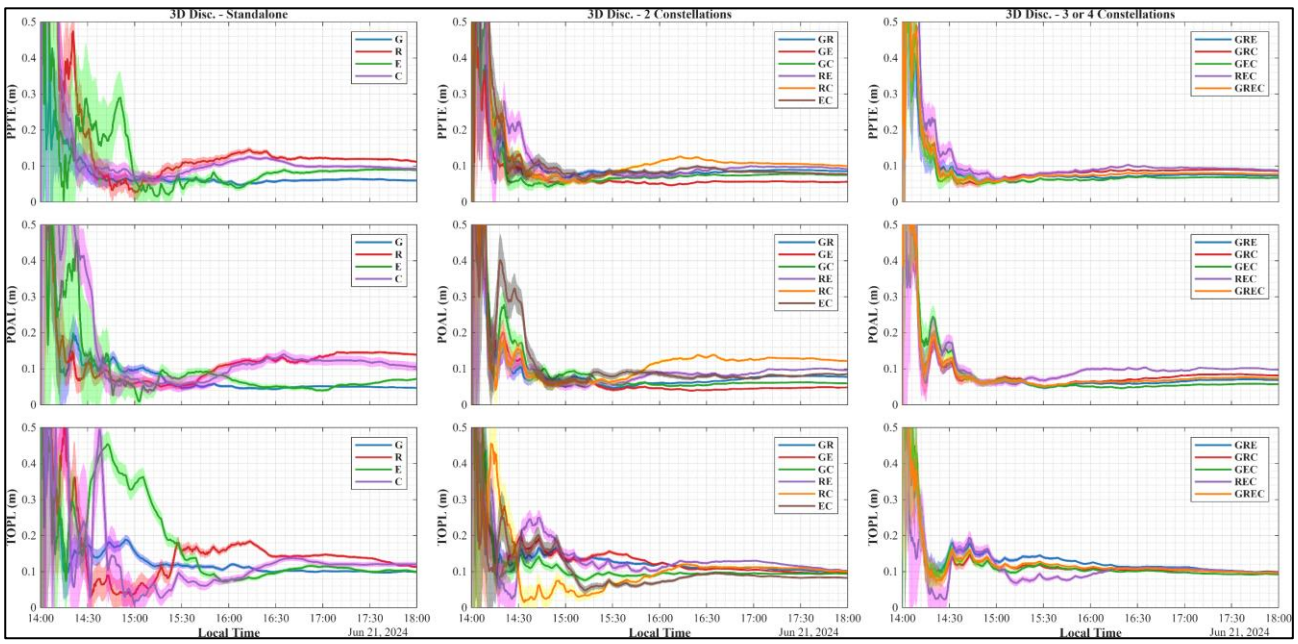

Figure 4. Evolution of 3D positional error, shadowed by standard deviation, over time for different GNSS constellation configurations on June 21, 2024. Results are shown for the stations PPTE (top), POAL (middle), and TOPL (bottom).

Regarding standalone solutions, GPS consistently delivered the best performance among the single-constellation configurations. After 4 hours, the average 3D discrepancy for GPS was 13.7 cm, followed by Galileo (18.5 cm) and GLONASS (20.4 cm). BeiDou, in contrast, exhibited the worst accuracy, with a mean error of 22.0 cm after 4 hours and 80.6 cm at 30 minutes. These results are coherent with the visibility analysis (Figure 3), which showed limited BeiDou tracking at POAL and TOPL due to receiver compatibility constraints. Despite the limitations, Galileo demonstrated promising accuracy across all stations, especially at TOPL where visibility was more favorable.

Triple- and quadruple-constellation combinations provided the best overall results. At PPTE, the combination GE achieved the lowest 3D discrepancy after 4 hours (9.6 cm), while GREC achieved the best performance at 30 minutes (32.0 cm). At POAL, GRE stood out across all collection intervals, with an improvement from 34.4 cm (30 min) to 10.9 cm (4 h), representing a 68% reduction in RMS. At TOPL, the best performance was obtained with GC and REC combinations, depending on the interval. Notably, REC achieved the best result at 30 minutes (30.2 cm), while GC delivered the lowest discrepancy after 4 hours (13.5 cm).

The mean 3D discrepancy (in centimetres), averaged across the three stations for each GNSS configuration and observation window, is summarized in Table 3. The results reinforce the trend of improvement with time and constellation diversity, while also highlighting the limitations of single-system solutions under shorter sessions.

This contribution has been peer-reviewed. The double-blind peer-review was conducted on the basis of the full paper.
https://doi.org/10.5194/isprs-annals-X-3-W4-2025-379-2026 | © Author(s) 2026. CC BY 4.0 License.

System	30min	1h	2h	4h
G	40.1	25.8	17.0	13.7
R	67.9	37.8	23.8	20.4
E	51.0	37.6	24.0	18.5
C	80.6	47.2	27.2	22.0
GR	36.6	23.2	16.1	13.6
GE	34.3	22.4	15.3	12.5
GC	39.9	24.5	15.9	13.1
RE	40.5	26.9	17.7	15.1
RC	50.3	28.7	18.0	16.0
EC	46.2	29.5	18.6	15.2
GRE	32.7	21.4	15.0	12.8
GRC	34.7	21.7	15.0	13.0
GEC	34.4	21.8	14.7	12.2
REC	37.6	24.4	16.1	14.1
GREC	32.0	20.6	14.4	12.4

Table 3. Average 3D positional accuracy (in centimetres) across the three stations (PPTE, POAL, TOPL), considering different GNSS combinations and data collection durations.

The performance of the full GREC combination stood out across all observation windows. Compared to the standalone GPS solution, the GREC configuration provided consistent improvements in 3D positional accuracy. For a 30-minute session, the average discrepancy decreased from 40.1 cm (GPS) to 32.0 cm with GREC, representing a 20.2% improvement. After 1 hour, the discrepancy was reduced from 25.8 cm to 20.6 cm, a 20.2% gain. In the 2-hour window, the improvement reached 15.3%, with values of 17.0 cm for GPS and 14.4 cm for GREC. Finally, after 4 hours of processing, the GREC solution achieved an accuracy of 12.4 cm, compared to 13.7 cm for GPS, corresponding to a 9.5% reduction in 3D RMS error.

These results demonstrate that even in short sessions, the integration of multiple constellations significantly enhances PPP accuracy, especially during the early convergence phase. Although the relative advantage of GREC decreases slightly with longer sessions—due to the stabilization of the filter—the multi-GNSS configuration continues to offer the most consistent and precise solutions across all tested scenarios.

5.2 Convergence Time

In addition to positional accuracy, the convergence time of the PPP solution was evaluated for both horizontal and vertical components. Convergence was defined as the first epoch at which the position error reached and then remained below 10 cm in the horizontal and 20 cm in the vertical component for at least 5 consecutive epochs. These thresholds reflect typical requirements for high-precision GNSS applications in geodesy and surveying. The convergence times obtained for each GNSS constellation combination across the three stations are shown in Figure 5.

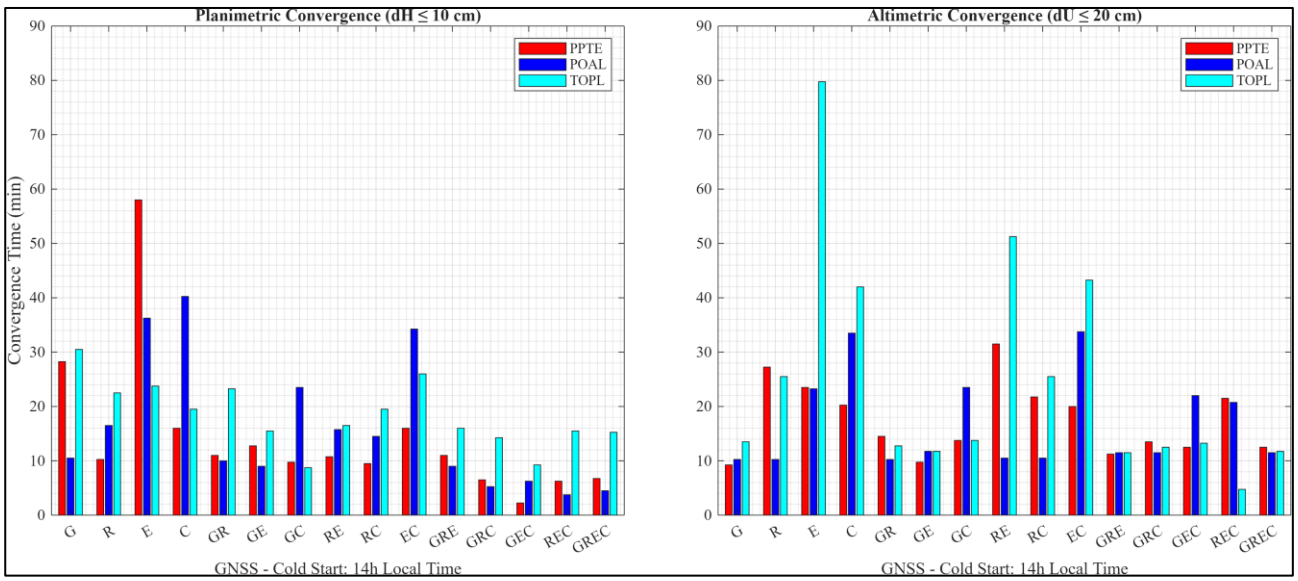

Figure 5. Convergence time for planimetric (left) and altimetric (right) components, for each GNSS constellation combination at stations PPTE (red), POAL (blue), and TOPL (cyan).

As expected, multi-constellation configurations led to faster convergence. The GREC solution consistently achieved the shortest convergence times in both components. On average, GREC reached horizontal convergence in less than 12 minutes and vertical convergence in approximately 20 minutes across all stations. Among the triple-constellation combinations, GEC and GRE also performed well, with convergence times close to GREC, especially at TOPL, which had higher satellite visibility.

Dual-constellation configurations showed intermediate performance, with convergence typically occurring between 15 and 30 minutes for the horizontal component. In contrast, single-constellation solutions presented longer convergence times, often exceeding 40 minutes in the vertical direction. GPS provided the best results among the standalone systems, while BeiDou presented the slowest convergence, with several cases exceeding the 1-hour mark or not converging within the observation window.

The results highlight the importance of integrating additional GNSS systems to accelerate solution convergence, particularly in environments with variable satellite visibility or challenging atmospheric conditions. Faster convergence not only enhances productivity in short-duration surveys but also contributes to improving the robustness and reliability of PPP solutions in real-time or near-real-time applications.

This contribution has been peer-reviewed. The double-blind peer-review was conducted on the basis of the full paper.
https://doi.org/10.5194/isprs-annals-X-3-W4-2025-379-2026 | © Author(s) 2026. CC BY 4.0 License.

6. Conclusion

The experimental evaluation demonstrated the effectiveness of APPPOLO in delivering accurate and reliable PPP solutions under various multi-GNSS configurations. The integration of constellations beyond GPS significantly enhanced both positional accuracy and convergence time, particularly in short observation windows. Among the tested combinations, triple- and quadruple-constellation configurations provided the best overall performance. The full GREC solution achieved sub-decimeter accuracy within 30 minutes, with improvements of up to 20% over standalone GPS in short sessions and nearly 10% after 4 hours. Among single-constellation solutions, GPS showed the most consistent results, while BeiDou presented limitations due to hardware constraints.

Convergence time analysis reinforced these findings. The GREC solution reached horizontal convergence in less than 12 minutes and vertical convergence in about 20 minutes at all stations. Multi-GNSS integration proved essential to accelerating convergence and improving solution robustness, especially under challenging or time-constrained conditions. In contrast, standalone configurations - particularly those relying solely on GLONASS or BeiDou - exhibited longer and more variable convergence behavior.

Overall, the results confirm that APPPOLO is capable of high-precision PPP processing and stands out for its modular, configurable structure and full support for multi-GNSS integration. These capabilities make it particularly suitable for advanced academic and operational applications in Brazil and elsewhere.

Based on the advances and limitations identified, several future research directions are proposed. First, the implementation of integer ambiguity resolution strategies for multi-GNSS PPP, especially using uncombined observations, would significantly enhance solution precision. The evaluation of real-time PPP techniques under short-duration sessions is also recommended to expand the method's applicability in practical contexts. Furthermore, the use of advanced atmospheric modeling - both empirical and numerical - should be explored to assess their influence on convergence and accuracy. High-rate data analysis and the assessment of ionospheric scintillation events remain essential to evaluate positioning performance under dynamic or extreme conditions. Lastly, the development of robust, adaptive quality control mechanisms is encouraged to ensure solution integrity in scenarios with degraded GNSS signals.

Acknowledgements

This study was financed, in part, by the São Paulo Research Foundation (FAPESP), Brasil. Process Number 2024/22757-0. The authors are also grateful to National Council for Scientific and Technological Development - CNPq (grant no. 306112/2023-0 and 130340/2023-5) This work is also part of consolidated national research initiatives, including the National Institute of Science and Technology (INCT) (CNPq Process 465548/2014-2) and the Public Policy Project "GNSS Technology for Supporting Air Navigation" (FAPESP Process 2017/50115-0).

References

Bahadur, B., Nohutcu, M., 2018. PPPH: A MATLAB-based software for multi-GNSS precise point positioning analysis. *GPS Solutions*, 22, 113. https://doi.org/10.1007/s10291-018-0777-z.

Blewitt, G., 1990. An automatic editing algorithm for GPS data. *Geophysical research letters* 17, no. 3 199-202.

Chen, K., Chang, X., 2021. PPPLib: An open-source software for precise point positioning using GPS, BeiDou, Galileo, GLONASS, and QZSS with multi-frequency observations. *GPS Solutions*, 25, 18. https://doi.org/10.1007/s10291-020-01052-4.

Choy, S., Bisnath, S., Rizos, C., 2017. Uncovering common misconceptions in GNSS Precise Point Positioning and its future prospect. *GPS Solutions*, 21. https://doi.org/10.1007/s10291-016-0545-x.

Geng, J., Guo, J., Xu, C., Deng, Z., Zhang, Y., Liu, J., 2019. PRIDE PPP-AR: an open-source software for GPS PPP with integer ambiguity resolution. GPS Solutions, 23, 91. https://doi.org/10.1007/s10291-019-0888-1.

Glaner, M.F., Weber, G., 2023. An open-source software package for Precise Point Positioning: raPPPid. *GPS Solutions* 27, 174 (2023). https://doi.org/10.1007/s10291-023-01488-4.

Kouba, J., Lahaye, F., Tétreault, P., 2017. Precise Point Positioning. In: Teunissen, P.J.G., Montenbruck, O. (Eds.), *Springer Handbook of Global Navigation Satellite Systems*. Springer, Berlin.

Montenbruck, O., Steigenberger, P., Prange, L., Deng, Z., Zhao, Q., Perosanz, F., Romero, I., Noll, C., Sturze, A., Weber, G., Schmid, R., Macleod, K, Schaer, S., 2017. The multi-GNSS experiment (MGEX) of the International GNSS Service (IGS) – achievements, prospects and challenges. *Advances in Space Research*, 59, 7. https://doi.org/10.1016/j.asr.2017.01.011.

Parvazi, K., Farzaneh, S. Safari, A., 2023. The mathematical weighting of GNSS observations based on different types of receivers/antennas and environmental conditions. *Geodesy and Geodynamics*, 14, 5. https://doi.org/10.1016/j.geog.2023.04.001.

Romero, I., 2021. RINEX – The Receiver Independent Exchange Format Version 4.00. *International GNSS Service* (IGS). Available at:https://files.igs.org/pub/data/format/rinex_4.00.pdf.

Takasu, T., 2013. *RTKLIB ver. 2.4.2 Manual*. Available at: http://www.rtklib.com.

Veettil, S. V., Aquino, M., Marques, H. A., Moraes, A., 2020. Mitigation of ionospheric scintillation effects on GNSS precise point positioning (PPP) at low latitudes. *Journal of Geodesy*, 94,15. https://doi.org/10.1007/s00190-020-01345-z.

Xiao, G., Liu, G., Ou, J., Liu, G., Wang, S., Guo, A., 2020. MG-APP: an open-source software for multi-GNSS precise point positioning and application analysis. *GPS Solutions* 24, 66. https://doi.org/10.1007/s10291-020-00976-1.

Zaupa, J.P.V., 2025. *Posicionamento por Ponto Preciso Multi-GNSS: Implementação e Análises*. M.Sc. Dissertation – Universidade Estadual Paulista (UNESP), Presidente Prudente.

Zhang, Q., Zhao, L., Zhao, L., Zhou, J., 2018. An Improved Robust Adaptive Kalman Filter for GNSS Precise Point Positioning. *IEEE Sensors Journal*, 18, 10. https://doi.org/10.1109/JSEN.2018.2820097.

Zhao, C., Zhang, B. & Zhang, X., 2021. SUPREME: an open-source single-frequency uncombined precise point positioning

software. *GPS Solutions* 25, 86. https://doi.org/10.1007/s10291-021-01131-0.

Zhou, F., Dong, D., Li, W., Jiang, X., Wickert, J., Schuh, H., 2018. GAMP: An open-source software of multi-GNSS precise point positioning using undifferenced and uncombined observations. *GPS Solutions* 22, 33. https://doi.org/10.1007/s10291-018-0699-9.

Zumberge, J.F., Heflin, M.B., Jefferson, D.C., Watkins, M.M., Webb, F.H., 1997. Precise point positioning for the efficient and robust analysis of GPS data from large networks. Journal of Geophysical Research: Solid Earth, 102(B3), 5005–5017. https://doi.org/10.1029/96JB03860.